Identification of a new p53 responsive element in the promoter region of anillin

JIAO MA[1], XINYING LIU[1], PENGYI LIU[1], WENQING LU[1], XINXIN SHEN[1], RUIXIANG MA[1] and HONGLIANG ZONG[2]

[1]Department of Biochemistry and Molecular Cell Biology, Shanghai Jiaotong University Medical School, Shanghai 200025; [2]Shanghai PerHum Therapeutics Co. Ltd., Shanghai 200052, P.R. China

Received June 13, 2019; Accepted December 6, 2019

DOI: 10.3892/ijmm.2020.4527

Abstract. The expression of anillin mRNA and protein is regulated in a cell cycle-dependent manner. However, the mechanism underlying this process is unclear. Previous studies analyzing the sequence of the 5'-untranslated region of anillin have unveiled several putative p53 binding sites. Therefore, the present study hypothesized that the anillin gene may be repressed by p53 and that the commonly observed mutation (or loss of function) of p53 may serve a role in this phenotype. Bioinformatic analysis of the anillin promoter region revealed potential p53 responsive elements. Of those identified, 2 were able to bind p53 protein, as determined via a chromatin immunoprecipitation assay. Although it was hypothesized that DNA damage and resultant p53 expression would repress anillin expression, the results revealed that anillin mRNA and protein expression levels were negatively regulated by DNA damage in the wild-type p53 cells, but not in the isogenic p53 null cells. Furthermore, DNA sequences encompassing the p53 binding site downregulated luciferase transgenes in a p53 dependent manner. Taken together, these data indicated that anillin was negatively regulated by p53 and that anillin overexpression observed in cancer may be a p53-mediated phenomenon. The data from the present study provided further evidence for the role of p53 in the biologically crucial process of cytokinesis.

Introduction

Anillin, an actin binding protein, serves crucial roles in cytokinesis. Anillin forms scaffolds upon which the actomyosin contractile ring forms and therefore functions as a central factor of the ingression and activity of the cleavage furrow (1-3). The transcription of the anillin (*ANLN)* gene locus and the resultant protein expression are cell cycle regulated (4). Furthermore, there are marked changes in localization during the cell cycle (5). In interphase cells, the anillin protein is restricted to the nucleus. However with the dissolution of the nuclear membrane at the onset of mitosis, anillin becomes phosphorylated (2) and relocates to the cell cortex, associating with the cell membrane prior to being accumulated at the developing cleavage furrow (5). Here, it serves as a scaffold, associating with actin (6), septins (7) myosin II (8) and also Rho like signaling complexes, including racGAP components (9) and a range of other proteins (10). The ubiquitin-mediated degradation of anillin, occurring at the end of mitosis, is facilitated by anaphase-promoting complex (11). The importance of anillin and anillin-associated proteins in cytokinesis has been demonstrated in several studies, including examining the effect of anillin mutations on cytokinesis (2,3,12). However, other functions of anillin in the nucleus or in association with other actomyosin activities including migration, cannot be excluded (13).

The coordinated and efficient execution of mitosis and cell division are important events that militate against oncogenic events associated with inaccurate or incorrect chromosome segregation and the mechanics of cell division (14). Therefore, it is not surprising that alterations in anillin expression have been described in neoplasia. Hall *et al* (15) performed global analyses of anillin in diverse samples of normal and diseased tissue, the results of which revealed that anillin overexpression occurred in neoplasia. Anillin mRNA is expressed at increased levels in human tumors. Furthermore, in many different types of tumor, a progressive increase in anillin mRNA levels has been associated with tumor spread and stage: For example, anillin is overexpressed in breast tumors, notably at the transition from *in situ* to invasive disease (16). Similarly, anillin has been demonstrated to be overexpressed in gastric carcinoma (17), pancreatic carcinomas (18), hepatocellular melanoma (19) and in head and neck squamous carcinoma (20). Further data from Suzuki *et al* (21) demonstrated anillin overexpression in lung cancer, which was associated with anillin dysfunction and perturbations of Rho and AKT signaling.

Correspondence to: Dr Jiao Ma, Department of Biochemistry and Molecular Cell Biology, Shanghai Jiaotong University Medical School, 280 South Chongqing Road, Shanghai 200025, P.R. China
E-mail: drjiaoma@shsmu.edu.cn

Dr Hongliang Zong, Shanghai PerHum Therapeutics Co. Ltd., 381 Middle Huaihai Road, Shanghai 200052, P.R. China
E-mail: zonghl@perhum.com

Key words: anillin, p53 putative binding sites, neoplasia, cytokinesis

The highly prevalent overexpression of anillin in multiple different types of tumors and its association with tumor progression is unusual and requires investigation. The increased expression of anillin is not a consequence of increased tumor growth fraction and it should be noted that the highest levels of anillin mRNA occur within the adult central nervous system, a tissue characterized by a non-proliferative phenotype (15). Furthermore, Mirza *et al* (22) demonstrated that a number of genes are repressed by p53, including anillin. Given the prevalence of p53 pathway defects in human cancer and previous evidence demonstrating that putative p53 binding sites are located within the 5'-untranslated region of the *ANLN* gene, the present study hypothesized that the tumor-associated loss of p53 function may negate its normally repressive effects on anillin expression. This would be consistent with the prevalence of anillin deregulation and with the association of increased anillin expression with tumor progression. The present study assessed the role of p53 in the regulation of anillin and demonstrated that anillin mRNA and protein may be regulated in a p53-dependent manner.

Materials and methods

The cancer genome Atlas (TCGA) database analysis. Anillin overexpression in patients with colorectal cancer was analyzed using data obtained from TCGA database (https://portal.gdc.cancer.gov/genes/ENSG00000011426). Anillin protein expression were analyzed in colorectal (n=239) or breast carcinomas (n=539) cases; normal colon (n=19) or breast tissues (n=61) were included as controls.

Bioinformatics. The upstream 3 kb region of the initiating ATG sequence was evaluated using UCSC Genome Browser software (http://www.genome.ucsc.edu) (23). Additionally, putative p53 responsive elements (REs) were identified using the online transcription factor prediction tool, Genomatix (http://www.genomatix.de/; Interxon Bioinformatics Germany GmbH).

Cell culture and transfection. p53 wild-type and isogenic p53 null HCT116 cells were donated by Dr B. Vogelstein (Oncology Center, Johns Hopkins University School of Medicine) and authentication was performed using the GenePrint10 system (Promega Corporation; cat. no. B9510). The MCF7 cell line was purchased from the American Type Culture Collection (cat. no. ATCC® HTB-22™). Cells were maintained at 37˚C in McCoy's 5A medium (Thermo Fisher Scientific, Inc.) under standard conditions and routinely tested for mycoplasma contamination using the MycAway-Color One-Step Mycoplasma detection kit [Yeasen Biotechnology (Shanghai) Co., Ltd.; cat. no. 40611ES60]. The full-length (-1 to -3,000), mutant A (-1,721 to-3,000) and mutant B (-2,105 to -3,000) constructs were cloned into pGL3 luciferase reporter vectors (cat. no. E1751; Promega Corporation). The transient transfection of these plasmids was then conducted for 48 h prior to western blotting to determine the transfection efficiency. HCT116 cells was subsequently performed using 24-well plates. Cells were grown at a density of ~1x10^5 cells/well in a 24-well plate 1 day prior to transfection. For each well, HCT116 $p53^{+/+}$ cells were co-transfected with 100 ng luciferase reporter plasmid and 20 ng β-galactosidase plasmid. HCT116 $p53^{-/-}$ cells were then co-transfected with 100 ng luciferase plasmids, 20 ng β-galactosidase plasmids and wild-type or mutant p53 (R175H or R248W) plasmids using GeneJuice® (Merck KGaA) according to the manufacturer's protocol.

Western blot analysis. HCT116 $p53^{+/+}$ or HCT116 $p53^{-/-}$ cells were treated with 0.5 μM doxorubicin for 0, 4, 12, 18, 24, 36 and 48 h. Cells were then lysed in RIPA buffer (50 mM Tris-base, 150 mM NaCl, 1% Triton X-100, 0.5% sodium deoxycholate, 0.5% SDS, 2 mM EDTA) and total protein was collected at 12, 18. 24 and 48 h time points. A total of 50 μg protein was electrophoresed on 8% SDS-PAGE gels, and semi-dry transferred to a PVDF membrane. Blots were then blocked in 2.5% milk for 30 min at room temperature, followed by incubation with either anillin S4 or mouse monoclonal p53 DO-1 antibodies (Santa Cruz Biotechnology, Inc.; cat. no. sc-126; 1:1,000) at 4˚C overnight. A goat anti-mouse horseradish peroxidase-conjugated IgG secondary antibody (Dako; Agilent Technologies, Inc; cat. no. P044701-2; 1:2,000) was then incubated with the PVDF membranes for 1 h at room temperature. ECL™ Western Blotting Detection Reagent (GE Healthcare Life Sciences) was then used to visualize the bands. Expression was quantified using ImageJ2 software (National Institutes of Health).

Reverse transcription-quantitative polymerase chain reaction (RT-qPCR). Total RNA (2 μg) extracted from HCT116 $p53^{+/+}$ and HCT116 $p53^{-/-}$ cells was reverse transcribed using M-MLV reverse transcriptase and random primers (Thermo Fisher Scientific, Inc.). qPCR was performed using SYBR-Green (cat. no. 04707516001; Roche Diagnostics) and the following gene-specific primers: Anillin, forward 5'-GAAAAGGTG ACCGAAAACCA-3', reverse 5'-TTTCGTCATTTCGCATT CAG-3'. Anillin mRNA level was normalized to β-actin (forward 5'-AGGCACCAGGGCGTGAT-3', reverse 5'-GCC CACATAGGAATCCTTCTGAC-3'). Amplification was performed in a LightCycler® 480 (Roche Diagnostics) using the following protocol: Initial denaturation at 95˚C for 5 min, followed by amplification at 95˚C for 10 sec and 72˚C for 30 sec for 40 cycles, and finally melting curve analysis at 95˚C for 5 sec, 65˚C for 1 min followed by cooling at 4˚C. An Opticon® 2 continuous fluorescence detection system equipped with Opticon® Monitor v2.02 software was also employed. The relative quantification cycle (C_q) method (24) was applied to analyze the relative expression of anillin.

Plasmid construction. Genomic DNA was prepared from HCT116 $p53^{+/+}$ cells for the construction of *ANLN* promoter-driven luciferase reporter plasmids. Reporter plasmids containing -1,318 (encoding the promoter region from -1,318 to -1, which included potential binding sites A and B), A (encoding the promoter region from -1,310 to -1, with a deletion from -901 to -561, excluding the binding site of B) and B (encoding the promoter region from -921 to -1, with a deletion from -661 to -561, excluding binding site A) regions were constructed into the *Xho*I/*Hin*dIII restriction sites of the pGL3-basic vector (Promega Corporation).

Chromatin immunoprecipitation (ChIP). MCF7 cells were cultured and treated as aforementioned. Chromatin

was sheared into 300-600 bp fragments using a bioruptor (Diagenode, Inc.) for 4 rounds of 10 cycles of 30 sec ON/30 sec OFF at 4˚C. Fragmented chromatin was centrifuged at 500 x g for 10 min at 4˚C to pellet the remaining insoluble material and the supernatant was pre-cleared overnight at 4˚C with 600 μl magnetic protein-G Dynal beads (Thermo Fisher Scientific, Inc.). The fragmented chromatin (50 μl) was reserved as an input control. The remaining chromatin fragments were precipitated overnight at 4˚C with magnetic protein-G beads bound with antibodies. For each ChIP reaction, either 10 μg anti-p53 DO1 antibody (Santa Cruz Biotechnology, Inc.; cat. no. sc-126; 1:1,000), 10 μg mouse IgG immunoglobulin (1:2,000; cat. no. R0480; Dako; Agilent Technologies, Inc.) or no antibody was added and incubated with 600 μl sheep anti-mouse IgG protein G (Dako; Agilent Technologies, Inc.) beads at 4˚C overnight. Beads were washed 8 times with RIPA buffer (50 mM HEPES at pH 8.0, 500 mM EDTA at pH 8.0, 10% NP-40, 10% Deoxycholate, 8 M LiCl, protease inhibitor cocktail) followed by 1 wash in 1 ml 1X TE buffer. Each reaction was transferred into a fresh 1.5 ml Eppendorf tube, and centrifuged at 1,000 x g for 3 min at 4˚C. Immune complexes were eluted with 50 μl elution buffer [10 mmol/l Tris-Cl (pH 8.0), 1% SDS, 5 mmol/l EDTA] at 65˚C for 10 min and pelleted at 14,000 x g for 30 sec. Supernatant was then transferred into a fresh 1.5 ml Eppendorf tube prior to elution with 120 μl elution buffer. Cross-links were reversed by incubating at 65˚C overnight. Eluted material was purified using a PCR clean up kit (Qiagen, Inc.). Promoter regions containing the potential p53 binding sites of A and B were amplified with GoTaq® DNA polymerase (cat. no. M3001; Promega Corporation) using the following site specific primers: p53a forward, 5'-GGAGGAATAGTTCTGTTTTG-3'; p53a reverse, 5'-TCTCCTGCTTATTCTTTGTA-3'; p53b forward, 5'-AAATTGTGCATGAACGCTT-3'; p53b reverse, 5'-TTGGCCTTCAGTAGCTTTG-3'; p53cd forward, 5'-GGGTCCCAGTTCAAGCAAT-3'. Amplification was performed in an Eppendorf Master cycler thermal cycler using the following temperature protocol: 95˚C for 5 min, followed by 95˚C for 30 sec, 55˚C for 1 min, 72˚C for 3 min 10 sec for 25 cycles, and then 72˚C for 5 min. PCR products were analyzed via electrophoresis on 1.5% agarose gels and visualized using ethidium bromide.

Luciferase reporter assay. HCT116 $p53^{+/+}$ and HCT116 $p53^{-/-}$ cells were cultured, treated and transfected as aforementioned. At 24 h post-transfection, cells were lysed in 1X passive lysis buffer on a shaker for 15 min at room temperature. Cells were pelleted via centrifugation at 14,000 x g for 5 min at 4˚C. Supernatants were subsequently transferred into corresponding tubes. Luciferase substrate stock solution was thawed to room temperature (22-26˚C) and the required quantity was diluted 1:2 in ddH_2O, and placed in foil-wrapped Sterilin™ (Thermo Fisher Scientific, Inc.) prior to use. A Luciferase Assay System (Promega Corporation; cat. no. E1500) was used and β-galactosidase (Roche Diagnostics; cat. no. 11291963103) activity was detected according to the manufacturers' protocols. The reaction was incubated at 37˚C for ~30 min until the color turned dark red. The activity was then assayed at 570 nm using a plate reader (Bio-Rad Laboratories, Inc.). Luciferase activity was normalized to *Renilla* luciferase activity (cat. no. E2231; Promega Corporation).

Statistical analysis. An unpaired Student's t-test was performed to compare the differences between two groups. A two-way analysis of variance followed by Tukey's multiple comparisons post hoc test was performed to compare the differences between the fold changes of anillin promoter luciferase activities with respect to p53 responsiveness. Statistical analysis was performed and graphs were generated by GraphPad prism v6.01 software (GraphPad, Software, Inc.). Data are presented as mean ± standard deviation of triplicate cultures and are representative of 3 independent experiments. $P<0.05$ was considered to indicate a statistically significant difference.

Results

Anillin serves as a biomarker of colorectal or breast cancer. Previous studies have demonstrated the overexpression of anillin in various types of tumors and its association with disease progression (16-19). To confirm its role as a biomarker, the present study assessed the expression of anillin using the TCGA database. The results revealed that anillin was highly expressed in the colorectal adenocarcinoma cohort (Fig. 1A; n=237) and the breast carcinoma cohort (Fig. 1B; n=593) when compared with the respective normal colon, rectum or breast tissues. Furthermore, its expression was increased in colorectal (Fig. 1C) or breast (Fig. 1D) tumors where tumor progression had been observed.

Bioinformatics analysis and ChIP identification of the putative p53 REs in the ANLN upstream 3 kb promoter. The classic p53 consensus DNA binding sequence contained the following: A half site of 5'-RRRCWWGYYY, a spacer consisting of 0-25 bases and a second half site of RRRCWWGYYY-3', where R represents purine, W represents adenine or thymidine, Y represents pyrimidine, G represents guanine and C represents cytosine. The 3 kb sequence located upstream of the ANLN promoter sequence was analyzed using Genomatix software, an online transcriptional factor prediction system. According to the classic p53 consensus DNA binding sequence, 4 putative p53 binding sites were identified and located (Fig. 2A): p53 RE-a, p53 RE-b, p53 RE-c and p53 RE-d. The sequences, the strand on which they were located and the start and ending positions of each p53 binding site are presented in Fig. 2B. By performing ChIP, the present study elucidated that sites p53 RE-a and -b were capable of binding p53 (Fig. 2C). However, other two putative binding sites, p53 RE-c/d, were not identified by the ChIP assay (Fig. S1). Mirza *et al* (22) previously demonstrated via a ChIP assay that RE-b was capable of binding p53 and repressed anillin expression. To further define the functionality of the anillin promoter with respect to p53 responsiveness, the present study constructed a series of luciferase reporter plasmids containing activated or mutated RE-a and/or RE-b (Figs. 2D and S2). Wild-type or p53 null counterparts containing either activated or mutated binding sites were subsequently transfected into the HCT116 cells. The results revealed that each site acted in *cis* to inhibit luciferase activity following doxorubicin treatment in a p53-dependent manner (Fig. 2E). By contrast, the inhibition of anillin

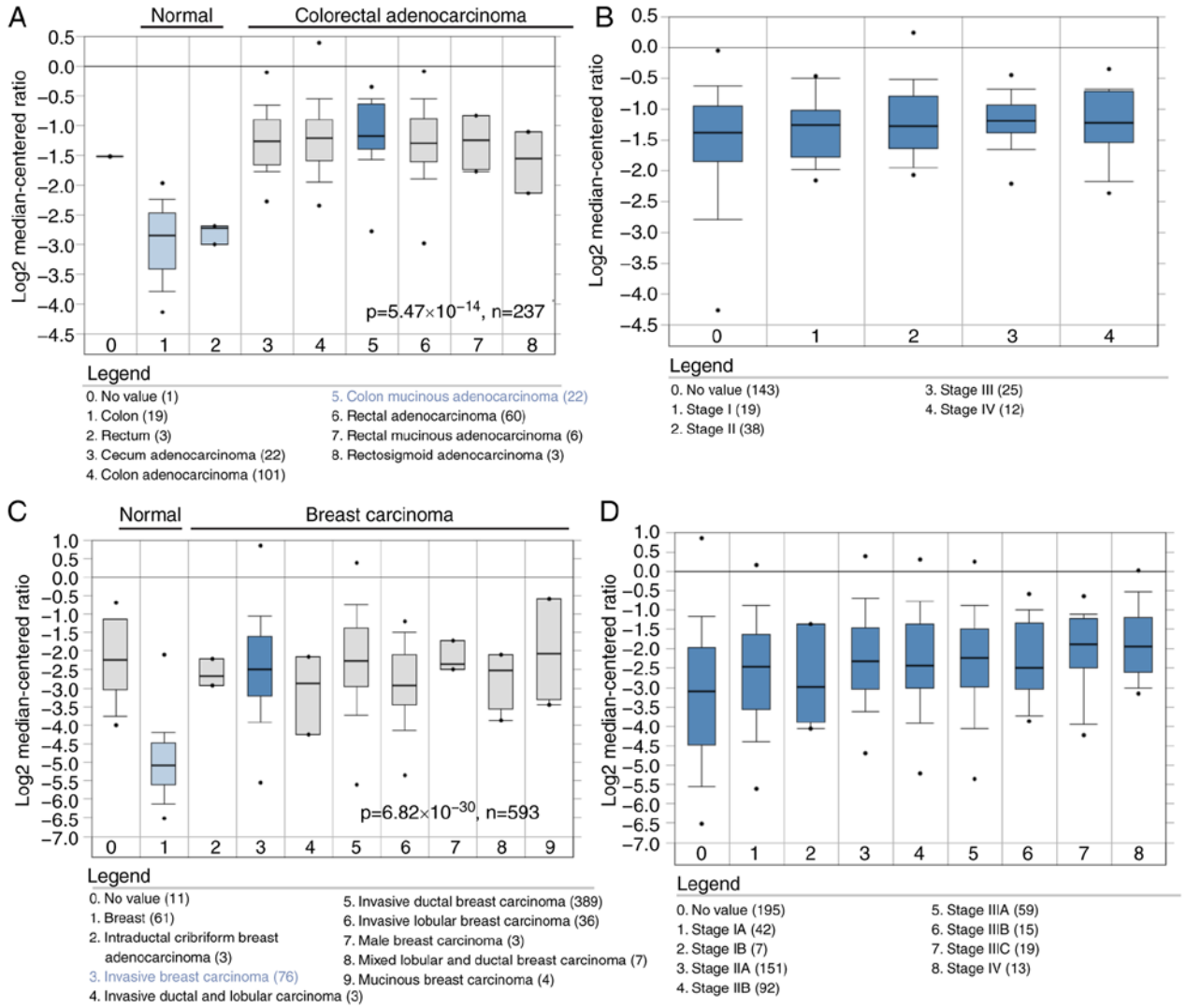

Figure 1. Anillin is overexpressed in colorectal and breast cancer, and its expression is often associated with the tumor progression. Anillin mRNA expressions in (A) normal tissue vs. colorectal carcinoma or (B) at different stages of colorectal cancer from TCGA colorectal database (n=237). Anillin mRNA expression levels in (C) normal tissue vs. breast carcinoma or (D) at different stages of breast cancer from TGCA breast database (n=593). An unpaired Student's t-test was performed to compare the differences between normal vs. cancer tissues. TGCA, The Cancer Genome Atlas.

promoter luciferase activities was negated by mutating the binding sites in the reporter plasmids (Fig. S2). In subsequent experiments, the constructs were co-transfected into p53-null cells with mutant or wild-type p53 constructs (Figs. 2F and S3). It was demonstrated that exogenous wild-type p53 repressed RE-a/b-containing luciferase constructs, while the mutants activated luciferase activity (Fig. 2F).

Repression of anillin mRNA and protein levels by the doxorubicin-induced accumulation of p53 in HCT116/p53$^{+/+}$ cells. To investigate whether anillin was regulated during apoptosis, HCT116/p53$^{+/+}$ cells were treated with doxorubicin to induce DNA damage. The results of the qPCR analysis revealed that anillin mRNA expression in HCT116/p53$^{+/+}$ cells was inhibited at 4 h after doxorubicin treatment (Fig. 3A). To confirm this result, cell lysates were collected at different time points following doxorubicin treatment and subjected to western blot analysis. The results revealed that the expression of anillin was downregulated in a time-dependent manner following doxorubicin treatment (Fig. 3B; top row). In addition, p53 expression was significantly increased following doxorubicin treatment (Fig. 3B; middle row), indicating that p53 may be involved in the regulation of anillin expression. Therefore, HCT116/p53$^{-/-}$ cells were treated with doxorubicin, following which qPCR and anillin western blot analysis were performed. Neither the qPCR nor western blot analysis assays revealed any alterations in anillin expression following doxorubicin treatment in the HCT116/p53$^{-/-}$ cells (Fig. 3C and D). These data indicated that p53 was a key transcription factor that regulated anillin expression during apoptosis.

Anillin expression is inhibited in p53-transfected HCT116/p53$^{-/-}$ cells. To additionally determine whether anillin functions a transcription factor to p53, 2 p53 mutants that were deficient in DNA-binding were employed. HCT116/p53$^{-/-}$ cells were transfected with wild-type or mutant p53 plasmids. The results of the qPCR analysis demonstrated that anillin mRNA overexpression was inhibited using the p53 wild-type construct. However, neither of the mutant constructs used in the present study (R175H or R248W) exerted an effect in

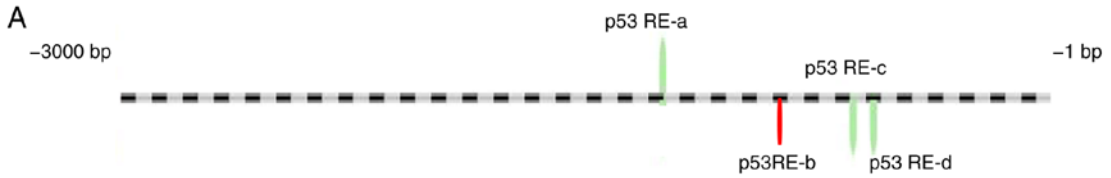

B

Putative p53 Responsive Elements (REs)	Sequence	Strand	Position start	Position end
p53 binding motif	***RRRCWWGYYY (N=0 to 25 bp) RRRCWWGYYY***	***Plus or minus***	***R=A or G***	***Y =C or T***
p53RE-a	AAT**CAAG**AAC tgtcatctttacctgcac AGA**CTTG**TTA	Plus	-1280	-1243
p53RE-b	AGG**CCTG**GCC ctcagaa AAG**CCAG**TTC	minus	-870	-896
p53RE-c	AGG**CATG**GTG GCG**CGTG**CCT	minus	-631	-650
p53RE-d	GTT**CAAG**ACC AGC**CTTG**CCA	minus	-566	-585

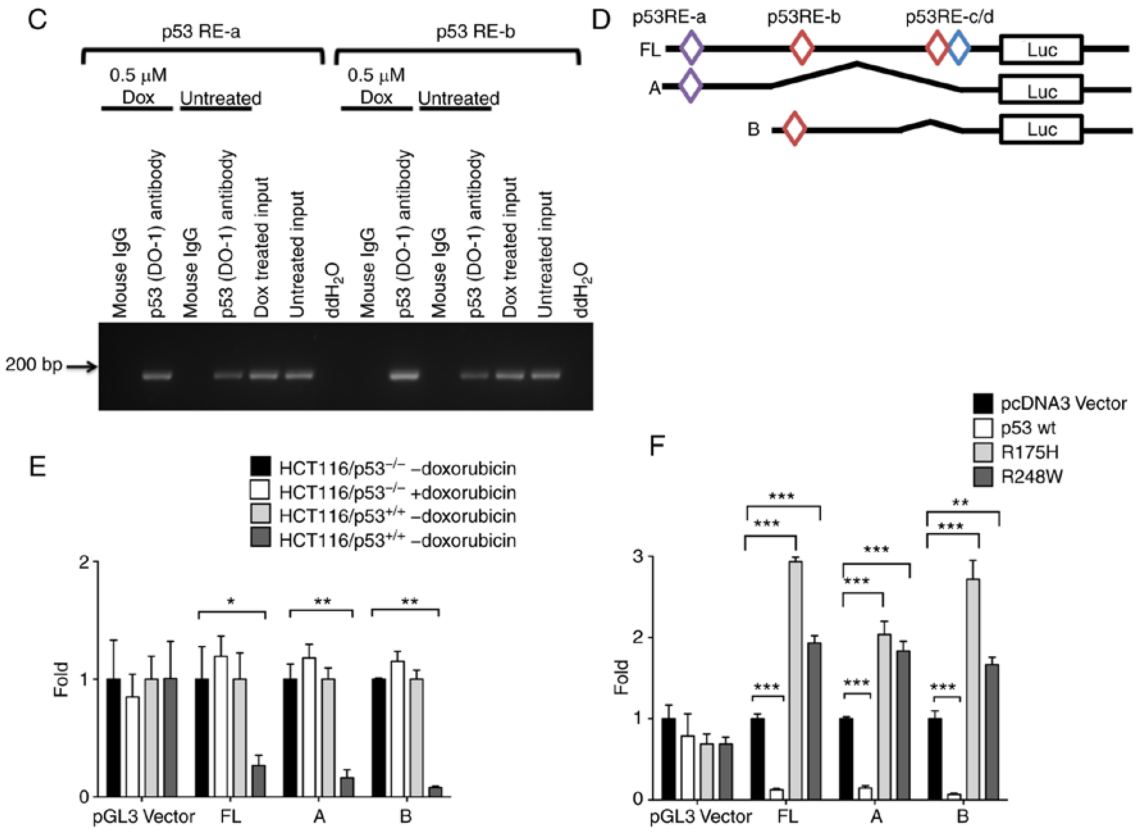

Figure 2. p53 directly binds to *ANLN* promoter to inhibit its transcription. (A) Schematic representation of the 4 putative p53 binding sites on *ANLN* 3 kb upstream promoter region. The striped line represents the *ANLN* upstream 3 kb promoter region. The 4 putative p53 REs were identified in this region. p53 RE-a started at -1,721 bp, with region a located at (+) strand of *ANLN* 3 kb region. In addition, p53 RE-c and p53 RE-d began at -2,351 bp and d started at -2,415 bp were closely located to each other on (-) strand. Therefore, they were grouped together as one region for the chromatin immunoprecipitation (ChIP) assay. The p53 RE-b of *ANLN*, represented by the red bar, started at -2,105 bp and was also included to confirm the results. (B) The p53 binding motif was included for comparison. The uppercase letters in bold represent the 4 core nucleotides of each half-site. The underlined and lowercase letters sequences represent mismatches to the consensus sequence. The half-site sequences separated from one another and from spacer nucleotides are indicated by a space. (C) MCF7 cells were treated with 0.5 μM doxorubicin. The chromatin immunoprecipitates were obtained using p53 antibody or mouse normal IgG, or without antibody, and analyzed using PCR. Chromatin inputs from doxorubicin-treated or non-treated MCF7 cells were also used as positive controls for PCR, while double-distilled H_2O was used as a PCR template for negative control. The PCR products were resolved on a 2% agarose gel. (D) Schematic representation of the *ANLN* promoter luciferase constructs. (E) β-galactosidase expression plasmids were co-transfected with the pGL3 vector or reporter plasmids FL, A or B into both HCT116/p53$^{+/+}$ and HCT116/p53$^{-/-}$ cells for 24 h. Cells were treated with 0.5 μM doxorubicin for an additional 24 h. Luciferase reporter activity was measured and normalized to β-galactosidase activity in the same sample, and presented as the fold decrease. (F) β-galactosidase expression plasmids were co-transfected with pGL3 vector or reporter plasmids FL, A or B, and pcDNA3, wild-type p53, R175H or R248W into HCT116/p53$^{-/-}$ cells. Luciferase reporter activity was measured after 24 h and normalized to β-galactosidase activity in the same sample, and presented as the fold decrease. The data are presented as the mean ± standard deviation of triplicate transfections, and are representative of 3 independent experiments. *P<0.05, **P<0.01 and ***P<0.001. ANLN, anillin; FL, full-length.

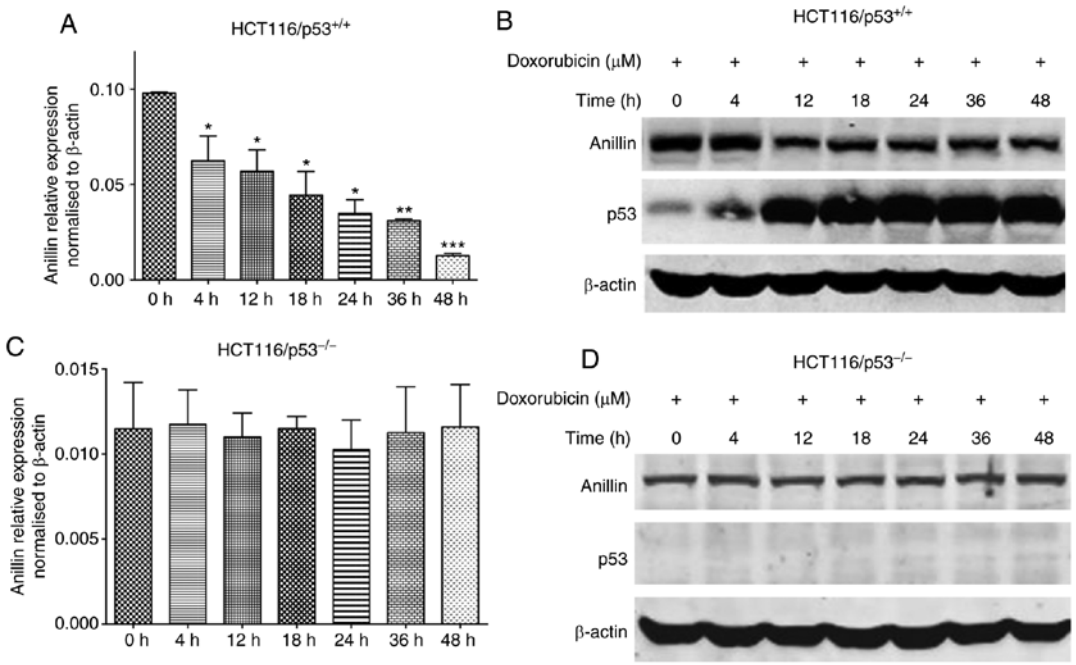

Figure 3. Anillin transcription and protein levels are repressed by p53 in a time-dependent manner. (A and B) HCT116/p53$^{+/+}$ and (C and D) HCT116/p53$^{-/-}$ cells were treated either with or without 0.5 μM doxorubicin at the indicated time points. RT-qPCR or western blot analysis were performed to detect anillin mRNA or protein expression using anillin S4 antiserum (B and D, top row) or p53 DO1 antibody (B and D, middle row). β-actin was included as a loading control. Data are presented as the mean ± SD of triplicate cultures and are representative of 3 independent experiments. *P<0.05, **P<0.01 and ***P<0.001 vs. non-treated cells.

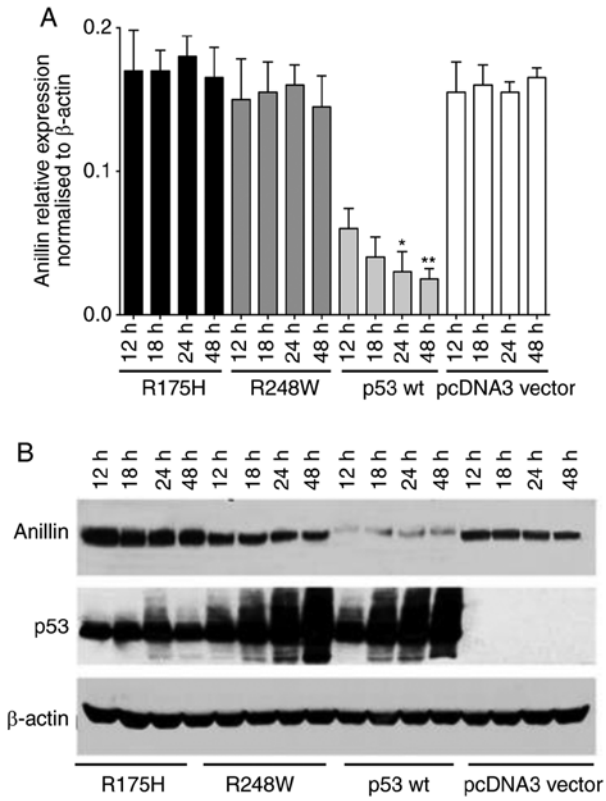

Figure 4. Expression of anillin mRNA and protein levels are repressed by wild-type p53, but not by dominant negative p53 mutants. R174H and R248W. HCT116/p53$^{-/-}$ cells were transfected with R175H, R248W wild-type or empty vectors. (A) Total RNA or (B) protein were extracted at different time points post-transfection, and subjected to (A) RT-qPCR or (B) western blot analysis using anillin S4 antiserum and a p53 DO1 antibody. β-actin was included as a loading control. Data are presented as the mean ± standard deviation of triplicate cultures, and are representative of 3 independent experiments. *P<0.05 and **P<0.01 vs. non-treated cells at corresponding time points. wt, wild-type.

HCT116/p53$^{-/-}$ cells (Fig. 4A). Additionally, anillin protein levels were suppressed by overexpressing p53 using the wild-type construct in HCT116 p53 null cells. However, no effect was observed in cells transfected with R175H or R248W p53 mutant constructs (Fig. 4B). These data indicated that p53 may regulate anillin transcription by directly binding to the *ANLN* promoter.

Discussion

By fulfilling the criteria set out by Riley *et al* (25), in which state that the p53 binding motif is composed of a half-site RRRCWWGYYY followed by a spacer (0-21 bp) and subsequently a second half-site RRRCWWGYYY sequence, the present study demonstrated that anillin may be a p53 responsive gene. This has relevance in 2 contexts: Firstly, the frequent overexpression of anillin in neoplasia and its association with tumor progression may be a consequence of p53 tumor suppressor gene loss of function, which itself is highly prevalent in human neoplasia and associated with tumor progression. This model was based on the suggestion that anillin was transcriptionally repressed by p53 and that p53 mutations may reverse this effect. The present data is consistent with the previously described model (24), since the potent transcriptional repression of the anillin promoter was induced by wild-type p53. This may explain why anillin overexpression is common in neoplasia and frequently associated with tumor progression.

The second inference made from the data of the present study is associated with the roles of p53 in cytokinesis. Cell cycle regulation of p53 expression has been well documented, despite the physiological role of this process being unclear (26). Previous studies have indicated the role of p53

in interphase and mitosis (27,28). It has been established that cytokinesis failure initiates the p53 pathway (29). However, emerging reports have demonstrated that certain p53 regulated genes have roles in cytokinesis, including protein regulator cytokinesis 1 (30,31). In addition, the p53-mediated regulation of the LIM domain kinase (LIMK2) splice variant *LIMK2b* links cell cycle checkpoint control with actin dynamics (32). Changes in cell shape are key processes in the cell cycle, and this is disrupted in incidences of neoplasia. Given the role of anillin as an actin interactor, it is hypothesized that the p53 dependent regulation of *ANLN* may modulate cytokinetic processes under conditions of cellular stress. Other studies have proposed an association between the p53 response and Septins, which are proteins that interact with anillin and have roles in cytokinesis (33,34).

Recent data have suggested associations between p53 and stem cell function and, in particular, between p53 and polarized asymmetric cell division (35,36). Anillin also serves roles across phylogeny in asymmetric cell divisions. In the development of *Caenorhabditis elegans,* protease-activated receptor 4 protein regulates polarity by altering the anillin scaffold and hence, actin and myosin dynamics (37). Similarly, anillin is crucial for the asymmetric divisions that give rise to polar bodies in nematode oocyte development (38). Asymmetric divisions are central to all eukaryote cell development (39), particularly in stem cell function. Evolutionary conservation of the structural and regulatory elements is also crucial for the determination of polarity (40).

Finally, the role of p53-regulated anillin expression may indicate the activities of anillin that are not involved with cytokinesis. Although the focus of the studies investigating anillin has been its significant roles in cytokinesis, substantial anillin protein levels have been observed in the interphase nucleus. While this may be a storage form of the protein (1,41), it may also indicate that anillin serves roles in regulating aspects of nuclear actin function (42). It is also notable that other cytokinesis proteins, including Pav and Tum, have important nuclear roles in the regulation of Wnt signaling (43). In addition to anillin, these proteins also interact with Rac GTPase-activating protein 1 (44). These observations, and the results of the present study, indicate that the scope of anillin function may be greater than previously considered.

Acknowledgements

The authors would like to thank Dr B. Vogelstein at Oncology Center, Johns Hopkins University School of Medicine for providing the p53 wild-type and isogenic p53 null HCT116 cells. The results shown in this manuscript are in part based upon data generated by the TCGA Research Network: https://www.cancer.gov/tcga.

Funding

This project was supported in part by Shanghai Pujiang Program (grant no. 17PJ1405500 to JM), Shanghai Natural Science Foundation (grant no. 17ZR1415600 to JM), and National Natural Science Foundation of China (grant no. 81700134 to JM).

Availability of data and materials

All data generated or analyzed during this study are included in this published article.

Authors' contributions

JM designed and performed the experiments, analyzed the data and wrote the manuscript. XL, RM, WL, XS and PL drafted parts of the manuscript. HZ conceived and supervised the project, designed the experiments and wrote the manuscript. All authors read and approved the final manuscript.

Ethics approval and consent to participate

Not applicable.

Patient consent for publication

Not applicable.

Competing interests

The authors declare that they have no competing interests.

References

1. Field CM and Alberts BM: Anillin, a contractile ring protein that cycles from the nucleus to the cell cortex. J Cell Biol 131: 165-178, 1995.
2. Kim H, Johnson JM, Lera RF, Brahma S and Burkard ME: Anillin phosphorylation controls timely membrane association and successful cytokinesis. PLoS Genet 13: e1006511, 2017.
3. Pollard TD and O'Shaughnessy B: Molecular mechanism of cytokinesis. Annu Rev Biochem 88: 661-689. 2019.
4. Zeng S, Yu X, Ma C, Song R, Zhang Z, Zi X, Chen X, Wang Y, Yu Y, Zhao J, *et al*: Transcriptome sequencing identifies ANLN as a promising prognostic biomarker in bladder urothelial carcinoma. Sci Rep 7: 3151, 2017.
5. Beaudet D, Akhshi T, Phillipp J, Law C and Piekny A: Active Ran regulates anillin function during cytokinesis. Mol Biol Cell 28: 3517-3531, 2017.
6. Zhang S, Nguyen LH, Zhou K, Tu HC, Sehgal A, Nassour I, Li L, Gopal P, Goodman J, Singal AG, *et al*: Knockdown of anillin actin binding protein blocks cytokinesis in hepatocytes and reduces liver tumor development in mice without affecting regeneration. Gastroenterology 154: 1421-1434, 2018.
7. Erwig MS, Patzig J, Steyer AM, Dibaj P, Heilmann M, Heilmann I, Jung RB, Kusch K, Möbius W, Jahn O, *et al*: Anillin facilitates septin assembly to prevent pathological outfoldings of central nervous system myelin. Elife 8: pii: e43888, 2019.
8. Yasuda T, Takaine M, Numata O and Nakano K: Anillin-related protein Mid1 regulates timely formation of the contractile ring in the fission yeast Schizosaccharomyces japonicus. Genes Cells 21: 594-607, 2016.
9. Gregory SL, Ebrahimi S, Milverton J, Jones WM, Bejsovec A and Saint R: Cell division requires a direct link between microtubule-bound RacGAP and anillin in the contractile ring. Curr Biol 18: 25-29, 2008.
10. Glotzer M: Cytokinesis in metazoa and fungi. Cold Spring Harb Perspect Biol 9: pii: a022343, 2017.
11. Zhao WM and Fang G: Anillin is a substrate of anaphase-promoting complex/cyclosome (APC/C) that controls spatial contractility of myosin during late cytokinesis. J Biol Chem 280: 33516-33524, 2005.
12. Perez AM and Thorner J: Septin-associated proteins Aim44 and Nis1 traffic between the bud neck and the nucleus in the yeast Saccharomyces cerevisiae. Cytoskeleton (Hoboken) 76: 15-32, 2019.
13. Wang D, Chadha GK, Feygin A and Ivanov AI: F-actin binding protein, anillin, regulates integrity of intercellular junctions in human epithelial cells. Cell Mol Life Sci 72: 3185-3200, 2015.

14. Stauffer S, Zeng Y, Zhou J, Chen X, Chen Y and Dong J: CDK1-mediated mitotic phosphorylation of PBK is involved in cytokinesis and inhibits its oncogenic activity. Cell Signal 39: 74-83, 2017.
15. Hall PA, Todd CB, Hyland PL, McDade SS, Grabsch H, Dattani M, Hillan KJ and Russell SE: The septin-binding protein anillin is overexpressed in diverse human tumors. Clin Cancer Res 11: 6780-6786, 2005.
16. Magnusson K, Gremel G, Rydén L, Pontén V, Uhlén M, Dimberg A, Jirström K and Pontén F: ANLN is a prognostic biomarker independent of Ki-67 and essential for cell cycle progression in primary breast cancer. BMC Cancer 16: 904, 2016.
17. Pandi NS, Manimuthu M, Harunipriya P, Murugesan M, Asha GV and Rajendran S: In silico analysis of expression pattern of a Wnt/β-catenin responsive gene ANLN in gastric cancer. Gene 545: 23-29, 2014.
18. Idichi T, Seki N, Kurahara H, Yonemori K, Osako Y, Arai T, Okato A, Kita Y, Arigami T, Mataki Y, *et al*: Regulation of actin-binding protein ANLN by antitumor miR-217 inhibits cancer cell aggressiveness in pancreatic ductal adenocarcinoma. Oncotarget 8: 53180-53193, 2017.
19. Lian YF, Huang YL, Wang JL, Deng MH, Xia TL, Zeng MS, Chen MS, Wang HB and Huang YH: Anillin is required for tumor growth and regulated by miR-15a/miR-16-1 in HBV-related hepatocellular carcinoma. Aging (Albany NY) 10: 1884-1901, 2018.
20. Shimizu S, Seki N, Sugimoto T, Horiguchi S, Tanzawa H, Hanazawa T and Okamoto Y: Identification of molecular targets in head and neck squamous cell carcinomas based on genome-wide gene expression profiling. Oncol Rep 18: 1489-1497, 2007.
21. Suzuki C, Daigo Y, Ishikawa N, Kato T, Hayama S, Ito T, Tsuchiya E and Nakamura Y: ANLN plays a critical role in human lung carcinogenesis through the activation of RHOA and by involvement in the phosphoinositide 3-kinase/AKT pathway. Cancer Res 65: 11314-11325, 2005.
22. Mirza A, Wu Q, Wang L, McClanahan T, Bishop WR, Gheyas F, Ding W, Hutchins B, Hockenberry T, Kirschmeier P, *et al*: Global transcriptional program of p53 target genes during the process of apoptosis and cell cycle progression. Oncogene 22: 3645-3654, 2003.
23. Kent WJ, Sugnet CW, Furey TS, Roskin KM, Pringle TH, Zahler AM and Haussler D: The human genome browser at UCSC. Genome Res 12: 996-1006, 2002.
24. Livak KJ and Schmittgen TD: Analysis of relative gene expression data using real-time quantitative PCR and the 2(-Delta Delta C(T)) method. Methods 25: 402-408, 2001.
25. Riley T, Sontag E, Chen P and Levine A: Transcriptional control of human p53-regulated genes. Nat Rev Mol Cell Biol 9: 402-412, 2008.
26. Zhong B, Shingyoji M, Hanazono M, Nguyễn TTT, Morinaga T, Tada Y, Hiroshima K, Shimada H and Tagawa M: A p53-stabilizing agent, CP-31398, induces p21 expression with increased G2/M phase through the YY1 transcription factor in esophageal carcinoma defective of the p53 pathway. Am J Cancer Res 9: 79-93, 2019.
27. Johmura Y and Nakanishi M: Multiple facets of p53 in senescence induction and maintenance. Cancer Sci 107: 1550-1555, 2016.
28. Luo Q, Guo H, Kuang P, Cui H, Deng H, Liu H, Lu Y, Wei Q, Chen L, Fang J, *et al*: Sodium fluoride arrests renal G2/M phase cell-cycle progression by activating ATM-Chk2-P53/Cdc25C signaling pathway in mice. Cell Physiol Biochem 51: 2421-2433, 2018.
29. Meitinger F, Anzola JV, Kaulich M, Richardson A, Stender JD, Benner C, Glass CK, Dowdy SF, Desai A, Shiau AK and Oegema K: 53BP1 and USP28 mediate p53 activation and G1 arrest after centrosome loss or extended mitotic duration. J Cell Biol 214: 155-166, 2016.
30. Zhang B, Shi X, Xu G, Kang W, Zhang W, Zhang S, Cao Y, Qian L, Zhan P, Yan H, *et al*: Elevated PRC1 in gastric carcinoma exerts oncogenic function and is targeted by piperlongumine in a p53-dependent manner. J Cell Mol Med 21: 1329-1341, 2017.
31. Tsuchihara K, Lapin V, Bakal C, Okada H, Brown L, Hirota-Tsuchihara M, Zaugg K, Ho A, Itie-Youten A, Harris-Brandts M, *et al*: Ckap2 regulates aneuploidy, cell cycling, and cell death in a p53-dependent manner. Cancer Res 65: 6685-6691, 2005.
32. Hsu FF, Lin TY, Chen JY and Shieh SY: p53-mediated transactivation of LIMK2b links actin dynamics to cell cycle checkpoint control. Oncogene 29: 2864-2876, 2010.
33. Patzig J, Erwig MS, Tenzer S, Kusch K, Dibaj P, Möbius W, Goebbels S, Schaeren-Wiemers N, Nave KA and Werner HB: Septin/anillin filaments scaffold central nervous system myelin to accelerate nerve conduction. Elife 5: pii: e17119, 2016.
34. Kremer BE, Adang LA and Macara IG: Septins regulate actin organization and cell-cycle arrest through nuclear accumulation of NCK mediated by SOCS7. Cell 130: 837-850, 2007.
35. Levine AJ, Puzio-Kuter AM, Chan CS and Hainaut P: The role of the p53 protein in stem-cell biology and epigenetic regulation. Cold Spring Harb Perspect Med 6: pii: a026153, 2016.
36. Itahana Y, Zhang J, Göke J, Vardy LA, Han R, Iwamoto K, Cukuroglu E, Robson P, Pouladi MA, Colman A and Itahana K: Histone modifications and p53 binding poise the p21 promoter for activation in human embryonic stem cells. Sci Rep 6: 28112, 2016.
37. Chartier NT, Salazar Ospina DP, Benkemoun L, Mayer M, Grill SW, Maddox AS and Labbé JC: PAR-4/LKB1 mobilizes nonmuscle myosin through anillin to regulate C. elegans embryonic polarization and cytokinesis. Curr Biol 21: 259-269, 2011.
38. Sharif B, Fadero T and Maddox AS: Anillin localization suggests distinct mechanisms of division plane specification in mouse oogenic meiosis I and II. Gene Expr Patterns 17: 98-106, 2015.
39. Fox S, Southam P, Pantin F, Kennaway R, Robinson S, Castorina G, Sánchez-Corrales YE, Sablowski R, Chan J, Grieneisen V, *et al*: Spatiotemporal coordination of cell division and growth during organ morphogenesis. PLoS Biol 16: e2005952, 2018.
40. Pillitteri LJ, Guo X and Dong J: Asymmetric cell division in plants: Mechanisms of symmetry breaking and cell fate determination. Cell Mol Life Sci 73: 4213-4229, 2016.
41. Oegema K, Savoian MS, Mitchison TJ and Field CM: Functional analysis of a human homologue of the Drosophila actin binding protein anillin suggests a role in cytokinesis. J Cell Biol 150: 539-552, 2000.
42. Gieni RS and Hendzel MJ: Actin dynamics and functions in the interphase nucleus: Moving toward an understanding of nuclear polymeric actin. Biochem Cell Biol 87: 283-306, 2009.
43. Jones WM, Chao AT, Zavortink M, Saint R and Bejsovec A: Cytokinesis proteins Tum and Pav have a nuclear role in Wnt regulation. J Cell Sci 123: 2179-2189, 2010.
44. Guillemot L, Guerrera D, Spadaro D, Tapia R, Jond L and Citi S: MgcRacGAP interacts with cingulin and paracingulin to regulate Rac1 activation and development of the tight junction barrier during epithelial junction assembly. Mol Biol Cell 25: 1995-2005, 2014.